CHAPTER 28

THE IRON II BURIAL CAVE: ANCIENT DNA SAMPLING AND ANALYSIS OF UNIPARENTAL MARKERS

Arie Shaus and David Reich

This chapter supplies basic DNA information regarding two individuals from the Iron II burial cave at Kiriath-jearim (Chapters 25, 26 and 27). Genetically these two individuals are one male (I14918) and one female (I14919). This data builds upon previously published materials (Shaus *et al.* 2023).

Materials and Methods

Two right petrous bones from two individuals, denoted here as I14918 and I14919 (and corresponding respectively to Individuals 4 and 2 in Chapter 27), were investigated. Images of sampled materials taken in the lab can be found in Figs. 28.1–28.2. In order to verify the chronological attribution (i.e., dismiss the possibility of intrusive materials), a small amount of material from I14918 was sent for ^{14}C dating. The outcome, calibrated using OxCal 4.4.2 (Bronk Ramsey 2009) and IntCal20 (Reimer *et al*. 2020), is 739–409 calBCE (2430±20 BP, PSUAMS-8559). This confirms the expected time span and is consistent with the pottery assemblage analysis in Chapter 26.

The petrous bones were processed in a dedicated ancient DNA cleanroom at Harvard Medical School. The powder was generated following a technique that uses a dental sandblaster to systematically locate, isolate and clean the cochlea (Pinhasi *et al*. 2019). The DNA was extracted following well-established protocols (Dabney *et al*. 2013; Korlevic *et al*. 2015; Rohland *et al*. 2018). Libraries (one for each sample) were prepared in a dual-indexed single-stranded mode (Gansauge *et al*. 2017; Gansauge *et al*. 2020). In order to reduce the rate of characteristic ancient DNA damage, the libraries were treated with uracil-DNA glycosylase (UDG) (Rohland *et al*. 2015), originating from *E. coli* (USER enzyme from NEB). DNA libraries were sequenced on an Illumina instrument following in-solution enrichment for sequences overlapping the mitochondrial genome and 1,233,013 genome-wide SNPs ("1240k"), and were bioinformatically processed as previously described (Fu *et al*. 2015; Mathieson *et al*. 2015; also see the custom processing pipeline at https://github.com/DreichLab/ADNA-Tools). Authenticity of the generated DNA data was satisfactory, assessed by the examining C-to-T substitutions at the end of the sequenced fragments (Rohland *et al*. 2015), mitochondrial DNA consensus sequence (Fu *et al*. 2013a), and estimates of X chromosome contamination (Korneliussen *et al*. 2014). Pseudo-haploid SNP calls were created by random sampling from overlapping reads.

mtDNA haplogroups were determined by aligning data (Li *et al*. 2009) of sufficient quality to the RSRS consensus genome (Behar *et al*. 2012). Following a construction of mitochondrial consensus sequences, haplogroups were determined using HaploGrep2 2.1.15 (Weissensteiner 2016) and Phylotree 17 (Van Oven 2015; https://www.phylotree.org). The match rate was estimated using contamMix 1.0–12 (Fu *et al*. 2013b).

Y chromosome haplogroups were determined using both on- and off-target sequences aligned to the Yfull 8.09 phylogenetic tree (https://www.yfull.com). The nomenclature used herein is that of the International Society of Genetic Genealogy (https://www.isogg.org) version 15.73.

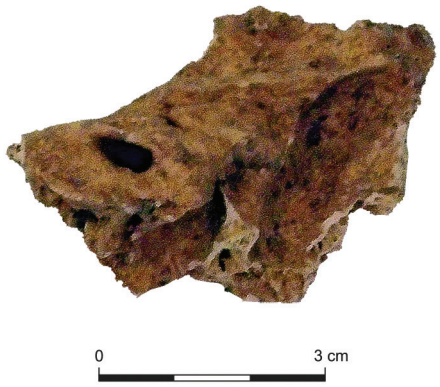

Fig. 28.1: Right petrous bone prior to sampling, Individual I14918

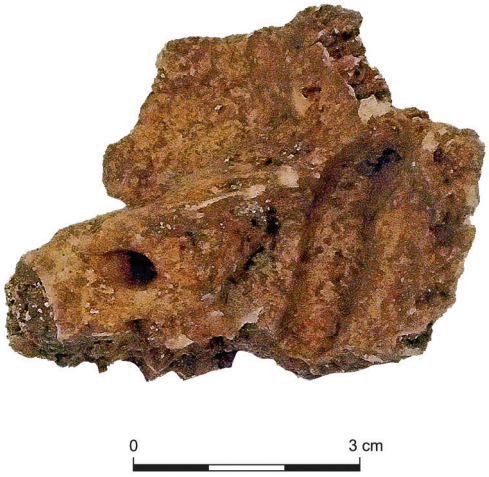

Fig. 28.2: Right petrous bone prior to sampling, Individual I14919

Results

In what follows, only information pertaining to uniparental markers (matrilineal mtDNA haplogroup and patrilineal Y chromosome haplogroup) are provided. An investigation of data from the whole genome will be the subject of a separate study as the analysis for this is complex and not yet complete.

A summary of the results for individuals I14918 and I14919 can be found in Table 28.1. The genetically determined sex (male for I14918 = Individual #4; and female for I14919 = Individual #2) corresponds to the anthropological analysis in Chapter 27. The autosomal coverage (closely tied to coverage on chromosome Y) and especially the mtDNA coverage are good. The mtDNA haplogroups are different, reflecting unrelated maternal lineages.

The uniparental haplogroups can be compared with previously published individuals, including modern and ancient DNA, utilizing information from Allen Ancient DNA Resource (AADR) V50.0 (https://reich.hms.harvard.edu/allen-ancient-dna-resource-aadr-downloadable-genotypes-present-day-and-ancient-dna-data).

In the following, no low coverage or potentially contaminated individuals are mentioned; in case several family members were published, the sample with the highest number of covered SNPs is shown.

Only one of our samples (I14918) possesses a Y chromosome. Nevertheless, the detected haplogroup, J2a1a1a2b2a1b1~ (the terminal "~" indicates a certainty that this is not one of the known J2a1a1a2b2a1b1 sub-haplogroups), is notable. As can be seen in Table 28.2, the ancestral J2a1 haplogroups are attested already in a Southern Caucasus hunter-gatherer individual in the eighth millennium BCE, and in a seventh millennium BCE individual in Anatolia. In the next millennia, various sub-haplogroups of J2a1a1a2b2a expand (perhaps in association with the spread of farming from Anatolia; cf. Lazaridis *et al*. 2016) into the

Table 28.1: Summary of basic information for individuals I14918 and I14919

ID	Skeletal element	Date (14C or estimation)	Sex	Autosomal coverage	Y haplogroup (ISOGG v15.73)	mtDNA haplogroup	mtDNA coverage
I14918 (Ind. #4)	right petrous	739–409 cal BCE (2430±20 BP, PSUAMS-8559)	M	1.463566	J2a1a1a2b2a1b1~	T1a9	193.7
I14919 (Ind. #2)	right petrous	750–650 BCE	F	1.30783	n/a (female)	H87	156.2

Table 28.2: Comparison with previously published material: Y haplogroups closest to J2a1a1a2b2a1b1~ (sub-haplogroups of J2a1a1a2b2a), as well as the oldest attestation of ancestral haplogroups J2a1 and J2a1a1a2b2; Marked in **bold—**individuals with haplogroups J2a1a1a2b2a1b1~ or sub-haplogroup J2a1a1a2b2a1b1b~

Version ID	Publication	Mean BP*	Group ID**	Y haplogroup (ISOGG v15.73)
KK1.SG	Jones *et al.* 2015	9,678	Georgia–Kotias.SG	J2a1
I0708	Mathieson *et al*. 2015	8,101	Turkey–N	J2a1
R19.SG	Antonio *et al.* 2019	7,146	Italy–N.SG	J2a1a1a2b2
I2056	Wang *et al.* 2019	6,466	Russia–Caucasus–Eneolithic	J2a1a1a2b2a3b1a~
I6268	Wang *et al.* 2019	5,550	Russia–Caucasus–Maikop–Novosvobodnaya	J2a1a1a2b2a3b~
ART022	Skourtanionti *et al.* 2020	5,413	Turkey–Arslantepe–LateC	J2a1a1a2b2a3b~
I6266	Wang *et al.* 2019	5,385	Russia–Caucasus–Maikop–Novosvobodnaya	J2a1a1a2b2a3b1a~
ART017	Skourtanionti *et al.* 2020	5,166	Turkey–Arslantepe–LateC	J2a1a1a2b2a2b2~
ART011	Skourtanionti *et al.* 2020	4,640	Turkey–Arslantepe–EBA	J2a1a1a2b2a3b1a1b~
ART001	**Skourtanionti *et al.* 2020**	**4,342**	**Turkey–Arslantepe–EBA**	**J2a1a1a2b2a1b1b~**
MA2205–final.SG	de Barros Damgaard *et al.* 2018	3,825	Turkey–AssyrianColonyPeriod.SG	J2a1a1a2b2a2b2b~
ALA011	Skourtanionti *et al*. 2020	3,620	Turkey–Alalakh–MLBA	J2a1a1a2b2a3b~
MA2200–final.SG	de Barros Damgaard *et al*. 2018	3,575	Turkey–OldHittitePeriod.SG	J2a1a1a2b2a2b2~

*Date mean in BP in years before 1950 CE (OxCal mu for a direct radiocarbon date, and average of range for a contextual date).
** No ending=1240k; SG=shotgun; DG=shotgun with diploid calling.

Table 28.2 (cont.)

Version ID	Publication	Mean BP*	Group ID**	Y haplogroup (ISOGG v15.73)
I11027	Narasimhan *et al*. 2019	3,526	Uzbekistan–Bustan–BA	J2a1a1a2b2a3b~
I4519	Agranat-Tamir *et al*. 2020	3,425	Israel–Megiddo–MLBA	J2a1a1a2b2a1a
I2190	Agranat-Tamir *et al*. 2020	3,351	Israel–Megiddo–MLBA	J2a1a1a2b2a1a
BR2.SG	Gamba *et al*. 2014	2,858	Hungary–LBA–Kyjatice.SG	J2a1a1a2b2a3b1a1b~
I14918	**(current)**	**2,477**	**Israel–KJ–IA**	**J2a1a1a2b2a1b1~**
R81.SG	Antonio *et al*. 2019	1,850	Italy–Imperial.SG	J2a1a1a2b2a2b2~
R115.SG	Antonio *et al*. 2019	1,850	Italy–Imperial.SG	J2a1a1a2b2a1a1c2~
R1550.SG	Antonio *et al*. 2019	1,814	Italy–Imperial–o4.SG	J2a1a1a2b2a1b1b~
R1551.SG	Antonio *et al*. 2019	1,797	Italy–Imperial–o3.SG	J2a1a1a2b2a3b1a1a2~
R44.SG	Antonio *et al*. 2019	1,750	Italy–Imperial.SG	J2a1a1a2b2a2b2b~
I3983	Olalde *et al*. 2019	1,550	Spain–Roman	J2a1a1a2b2a2b3a
I12220–published	Fernandes *et al*. 2020	1,306	Italy–Sardinia–LA	J2a1a1a2b2a1a1c1a~
R969.SG	**Antonio *et al*. 2019**	**300**	**Italy–EarlyModern.SG**	**J2a1a1a2b2a1b1~**
S–French-1.DG	Mallick *et al*. 2016	0	French.DG	J2a1a1a2b2a1a1a~
HG02236.SG	1KG *et al*. 2015	0	IBS.SG [Iberia, Spain]	J2a1a1a2b2a3b~
HG01402.SG	1KG *et al*. 2015	0	PUR.SG [Puerto Rico]	J2a1a1a2b2a3b1a1b1~
S–Abkhasian-2.DG	Mallick 2016	0	Russia–Abkhasian.DG	J2a1a1a2b2a3b1a1a2~
S–North–Ossetian-2.DG	Mallick 2016	0	Russia–NorthOssetian.DG	J2a1a1a2b2a3a1~
S–Samaritan-1.DG	Mallick *et al*. 2016	0	Samaritan.DG	J2a1a1a2b2a3b1a1b1a2~
NA20513.SG	1KG *et al*. 2015	0	TSI.SG [Tuscany, Italy]	J2a1a1a2b2a1a1~
NA20521.SG	1KG *et al*. 2015	0	TSI.SG	J2a1a1a2b2a2b3a
NA20534.SG	1KG *et al*. 2015	0	TSI.SG	J2a1a1a2b2a3b1b~
NA20765.SG	1KG *et al*. 2015	0	TSI.SG	J2a1a1a2b2a1a1a2a~
NA20787.SG	1KG *et al*. 2015	0	TSI.SG	J2a1a1a2b2a2b3a
NA20801.SG	1KG *et al*. 2015	0	TSI.SG	J2a1a1a2b2a2b3a
NA20815.SG	1KG *et al*. 2015	0	TSI.SG	J2a1a1a2b2a1a1~
NA20827.SG	1KG *et al*. 2015	0	TSI.SG	J2a1a1a2b2a1a1~
S–Tuscan-2.DG	Mallick *et al*. 2016	0	Tuscan–1.DG	J2a1a1a2b2a1a1a2a~

Central Mediterranean, the Levant and even to Central Asia. This (undoubtedly incomplete) information indicates that BCE, the lion's share of the J2a1a1a2b2a sub-haplogroups were concentrated in the Northern Caucasus, Anatolia and the Levant, including Alalakh in the Middle Bronze Age and Megiddo in the Late Bronze Age. Only in the last two millennia (CE), such sub-haplogroups can be found in large clusters in the Central and Western Mediterranean, but also in the Northern Caucasus, in Israel (in a modern-day Samaritan), and as remotely as in Puerto Rico. Interestingly, the only individual possessing a haplogroup identical to I14918 (J2a1a1a2b2a1b1~) is an early modern individual from Italy (R969.SG); on the other hand, already in Early Bronze Age Anatolia (individual ART001), we can observe a sub-haplogroup J2a1a1a2b2a1b1b~, indicating a relatively early appearance of J2a1a1a2b2a1b1~ itself.

The mtDNA haplogroups are also of interest. As can be seen in Table 28.3, haplogroup T1a9, observed in Individual I14918, also has close counterparts in the published ancient DNA literature. Indeed, its ancestral haplogroup T1a can be seen in the sixth–fifth millennia BCE in Southeastern Europe. Individuals possessing a sister haplogroup T1a2 can be seen in ʻAin Ghazal in Jordan already during PPNB, ca. 8000 BCE. These two facts may indicate a rather ancient source of T1a, perhaps (again) in Anatolia or the Levant. Later instances

Table 28.3: Comparison with previously published material: mtDNA haplogroups closest to T1a9 ~ (sub-haplogroups of T1a)—their oldest attestations, as well as all of the attestations of ancestral haplogroup T1a; Marked in **bold**—individuals with haplogroups T1a9

Version ID	Publication	Mean BP*	Group ID**	mtDNA haplogroup
I1700–published	Lazaridis *et al*. 2016	10,050	Jordan–ʻAinGhazal–PPNB	T1a2
I1415–published	Lazaridis *et al*. 2016	9,827	Jordan–ʻAinGhazal–PPNB	T1a2
I2529–published	Mathieson *et al*. 2018	7,610	Bulgaria–N	T1a
I1882	Lipson *et al*. 2017	7,050	Hungary–MN–LBK	T1a
I0447–published	Lipson *et al*. 2017	6,700	Hungary–LN–Tisza	T1a
I3708	Mathieson *et al*. 2018	6,500	Greece–Peloponnese–N	T1a
I10274	Novak *et al*. 2021	6,050	Croatia–C–Lasinja	T1a1
I1182	Harney *et al*. 2018	5,950	Israel–Pkiʻin–C	T1a+152
I11476	Narasimhan *et al*. 2019	4,600	Iran–BA1–ShahrISokhta	T1a3
I10264	Agranat-Tamir *et al*. 2020	3,750	Israel–Megiddo–MLBA	T1a
ALA026	Skourtanionti *et al*. 2020	3,627	Turkey–Alalakh–MLBA	T1a
I10097	Agranat-Tamir *et al*. 2020	3,500	Israel–Megiddo–MLBA	T1a
s19–X02–1.SG	Saag *et al*. 2019	2,937	Estonia–BA.SG	T1a1b
MJ-42.SG	Jarve *et al*. 2019	2,604	Russia–EasternScythian–SouthernUrals.SG	T1a1d
I14918	**(current)**	**2,477**	**Israel–KJ–IA**	**T1a9**
R131.SG	Antonio *et al*. 2019	1,850	Italy–Imperial.SG	T1a12
PCA0093	**Stolarek *et al*. 2012**	**1,700**	**Poland–IA–Gothic.mtDNA**	**T1a9**
VK147.SG	Margaryan *et al*. 2020	1,010	England–Viking.SG	T1a1q
VK435.SG	Margaryan *et al*. 2020	975	Sweden–Viking.SG	T1a5a
vik–nuf002.SG	Krzewinska *et al*. 2018	900	Sweden–Viking.SG	T1a1j
VK535.SG	Margaryan *et al*. 2020	700	Italy–Medieval.SG	T1a5

* Date mean in BP in years before 1950 CE (OxCal mu for a direct radiocarbon date, and average of range for a contextual date).
** Main analysis: no ending=1240k; SG=shotgun; mtDNA=mtDNA only.

of sub-haplogroups of T1a include a Chalcolithic individual from Pkiʿin in Israel; Bronze Age individual from Shahr-i Sokhta in Eastern Iran; and Middle Bronze Age Levantine individuals from Alalakh and Megiddo. After 1000 BCE, we can observe a larger geographic spread, including (apart from Kiriath-jearim) the Baltics, the Ural Mountains, the Central Mediterranean and Northern Europe. An exact match to T1a9 can only be found in individual (PCA0093) found in a late Iron Age Polish site attributed to the Goths (Stolarek *et al.* 2019).

Haplogroup H87, observed in Individual I14919, has no analogs in the published ancient DNA literature as of today. However, the exact haplogroup was observed in the following modern populations: Basques (Young 2009); Tunisian Arabs (Elkamel *et al*. 2018) and Iraqis (Shneewer *et al*. 2015). This may provide an indication of Mediterranean or Near Eastern, perhaps Arabian Peninsula source of the haplogroup. For the sake of completeness, it can also be added that (Behar *et al*. 2012) date the appearance of H87 to 5678.6 BP. However, with standard deviation (SD) of 5583, this estimate is highly non-specific.

Summary

This short report supplies basic information regarding two individuals from the Iron II burial cave at Kiriath-jearim. Genetically these are one male (I14918) and one female (I14919). Our analysis concentrated on patrilineal (Y haplogroup) and matrilineal (mtDNA haplogroups) markers. Upon comparison to other published material, the haplogroups appear to be of broadly "local" geographic span and possibly rather ancient origin. Y haplogroup J2a1a1a2b2a1b1~ probably originated in the Caucasus or Anatolia, perhaps as early as the late Upper Paleolithic. mtDNA haplogroup T1a9 may have been present in the Near East in PPN, and H87 might have its roots in the Arabian Peninsula. Moreover, we can cautiously observe that their ancestral, cladal and sub-haplogroups continued to exist, mainly in the Near East and the Mediterranean for many millennia, with geographically proximate examples at sites such as ʿAin Ghazal in PPNB; Chalcolithic Pkiʿin; and Middle–Late Bronze Megiddo and Alalakh; these haplogroups persist to the present day.

As noted above, this report did not explore the challenging wealth of autosomal data obtained from these individuals; this analysis will be provided in a subsequent publication. The excellent quality of the data also suggests that non-cranial osteologic materials from other individuals mentioned in Chapter 27 might yield beneficial paleogenomic data. Future attempts on these samples might be worthwhile despite the overall low rate of preservation of DNA in skeletal materials from ancient Israel.

References

1000 Genomes Project Consortium, Auton, A., Brooks, L.D., Durbin, R.M., Garrison, E.P., Kang, H.M., Korbel, J.O., Marchini, J.L., McCarthy, S., McVean, G.A. and Abecasis, G.R. 2015. A Global Reference for Human Genetic Variation. *Nature* 526(7571): 68–74.

Agranat-Tamir, L., Waldman, S., Martin, M.A.S., *et al.* 2020. The Genomic History of the Bronze Age Southern Levant. *Cell* 181(5): 1146–1157.

Antonio, M.L., Gao, Z., Moots, H.M., *et al.* 2019. Ancient Rome: A Genetic Crossroads of Europe and the Mediterranean. *Science* 366(6466): 708–714.

Behar, D.M., Van Oven, M., Rosset, S., Metspalu, M., Loogväli, E.-L., Silva, N.M., Kivisild, T., Torroni, A. and Villems, R. 2012. A "Copernican" Reassessment of the Human Mitochondrial DNA Tree from Its Root. *American Journal of Human Genetics* 90: 675–684.

Bronk Ramsey, C. 2009. Bayesian Analysis of Radiocarbon Dates. *Radiocarbon* 51: 337–360.

Dabney, J., Knapp, M., Glocke, I., Gansauge, M.-T., Weihmann, A., Nickel, B., Valdiosera, C., García, N., Pääbo, S., Arsuaga, J.-L. and Meyer, M. 2013. Complete Mitochondrial Genome Sequence of a Middle Pleistocene Cave Bear Reconstructed from Ultrashort DNA Fragments. *Proceedings of the National Academy of Sciences of the United States of America* 110: 15758–15763.

de Barros Damgaard, P., Martiniano, R., Kamm, J., *et al.* 2018. The First Horse Herders and the Impact of Early Bronze Age Steppe Expansions into Asia. *Science* 360(6396): eaar7711.

Elkamel, S., Boussetta, S., Khodjet-El-Khil, H., Benammar Elgaaied, A. and Cherni, L. 2018. Ancient and Recent Middle Eastern Maternal Genetic Contribution to North Africa as Viewed by mtDNA Diversity in Tunisian Arab Populations. *American Journal of Human Biology* e23100.

Fernandes, D.M., Mittnik, A., Olalde, I., *et al.* 2020. The Spread of Steppe and Iranian-related Ancestry in the Islands of the Western Mediterranean. *Nature Ecology and Evolution* 4(3): 334–345.

Fu, Q., Meyer, M., Gao, X., Stenzel, U., Burbano, H.A., Kelso, J. and Pääbo, S. 2013a. DNA Analysis of an Early Modern Human from Tianyuan Cave, China. *Proceedings of the National Academy of Sciences of the United States of America* 110: 2223–2227.

Fu, Q., Mittnik, A., Johnson, P.L.F., Bos, K., *et al.* 2013b. Revised Timescale for Human Evolution Based on Ancient Mitochondrial Genomes. *Current Biology* 23: 553–559.

Gamba, C., Jones, E.R., Teasdale, M.D., McLaughlin, R.L., *et al.* 2014. Genome Flux and Stasis in a Five Millennium Transect of European Prehistory. *Nature Communications* 5: 5257.

Gansauge, M.-T., Gerber, T., Glocke, I., Korlevic, P., Lippik, L., Nagel, S., Riehl, L.M., Schmidt, A. and Meyer, M. 2017. Single-stranded DNA Library Preparation from Highly Degraded DNA Using T4 DNA Ligase. *Nucleic Acids Research* 45(10): e79–e79.

Gansauge, M.-T., Aximu-Petri, A., Nagel, S. and Meyer, M. 2020. Manual and Automated Preparation of Single-stranded DNA Libraries for the Sequencing of DNA from Ancient Biological Remains and Other Sources of Highly Degraded DNA. *Nature Protocols* 15: 2279–2300.

Harney, É., May, H., Shalem, D., *et al.* 2018. Ancient DNA from Chalcolithic Israel Reveals the Role of Population Mixture in Cultural Transformation. *Nature Communications* 9(1): 3336.

Järve, M., Saag, L., Scheib, C.L., *et al.* 2019. Shifts in the Genetic Landscape of the Western Eurasian Steppe Associated with the Beginning and End of the Scythian Dominance. *Current Biology* 29(14): 2430–2441.

Jones, E.R., Gonzalez-Fortes, G., Connell, S., *et al.* 2015. Upper Palaeolithic Genomes Reveal Deep Roots of Modern Eurasians. *Nature Communications* 6: 8912.

Korlević, P., Gerber, T., Gansauge, M.-T., Hajdinjak, M., Nagel, S., Aximu-Petri, A. and Meyer, M. 2015. Reducing Microbial and Human Contamination in DNA Extractions from Ancient Bones and Teeth. *BioTechniques* 58: 87–93.

Korneliussen, T.S., Albrechtsen, A. and Nielsen, R. 2014. ANGSD: Analysis of Next Generation Sequencing Data. *BMC Bioinformatics* 15: 356.

Krzewińska, M., Kjellström, A., Günther, T., *et al.* 2018. Genomic and Strontium Isotope Variation Reveal Immigration Patterns in a Viking Age Town. *Current Biology* 28(17): 2730–2738.

Lazaridis, I., Nadel, D., Rollefson, G., *et al.* 2016. Genomic Insights into the Origin of Farming in the Ancient Near East. *Nature* 536(7617): 419–424.

Li, H., Handsaker. B., Wysoker, A., Fennell, T., Ruan, J., Homer, N., Marth, G., Abecasis, G. and Durbin, R. 2009. 1000 Genome Project Data Processing Subgroup. *Bioinformatics* 25: 2078–2079.

Lipson, M., Szécsényi-Nagy, A., Mallick, S., Pósa, A., *et al.* 2017. Parallel Palaeogenomic Transects Reveal Complex Genetic History of Early European Farmers. *Nature* 551(7680): 368–372.

Mallick, S., Li., H., Lipson, M., *et al.* 2016. The Simons Genome Diversity Project: 300 Genomes from 142 Diverse Populations. *Nature* 538(7624): 201–206.

Margaryan, A., Lawson, D.J., Sikora, M., *et al.* 2020. Population Genomics of the Viking World. *Nature* 585(7825): 390–396.

Mathieson, I., Lazaridis, I., Rohland, N., *et al.* 2015. Genome-wide Patterns of Selection in 230 Ancient Eurasians. *Nature* 528(7583): 499–503.

Mathieson, I., Alpaslan-Roodenberg, S., Posth, C., *et al.* 2018. The Genomic History of Southeastern Europe. *Nature* 555(7695): 197–203.

Narasimhan, V.M., Patterson, N., Moorjani, P., *et al.* 2019. The Formation of Human Populations in South and Central Asia. *Science* 365(6457): eaat7487.

Novak, M., Olalde, I., Ringbauer, H., Rohland, N., Ahern, J., Balen, J., Janković, I., Potrebica, H., Pinhasi, R. and Reich, D. 2021. Genome-Wide Analysis of Nearly all the Victims of a 6200 Year Old Massacre. *PLoS ONE* 16(3): e0247332.

Olalde, I., Mallick, S., Patterson, N., *et al.* 2019. The Genomic History of the Iberian Peninsula over the Past 8000 Years. *Science* 363(6432): 1230–1234.

Reimer, P., Austin, W.E.N., Bard, E., *et al.* 2020. The IntCal20 Northern Hemisphere Radiocarbon Age Calibration Curve (0–55 kcal BP). *Radiocarbon* 62(4): 725–757.

Rohland, N., Harney, E., Mallick, S., Nordenfelt, S. and Reich, D. 2015. Partial Uracil–DNA–Glycosylase Treatment for Screening of Ancient DNA. *Philosophical Transactions of the Royal Society of London. Series B, Biological Sciences* 370: 20130624.

Saag, L., Laneman, M., Varul, L., *et al.* 2019. The Arrival of Siberian Ancestry Connecting the Eastern Baltic to Uralic Speakers Further East. *Current Biology* 29(10): 1701–1711.

Shaus, A., Reich, D., Goldenberg, G., Freud, L., Eshed, V. and Finkelstein, I. 2023. Ancient Mitochondrial DNA Analysis of an Iron II Burial Cave on the Slope of Tel Kiriath-Yearim. In: Shalev, Y., Peleg-Barkat, O., Zelinger, Y. and Gadot. Y., eds. *New Studies in the Archaeology of Jerusalem and Its Region Collected Papers, Vol. XVI*. Jerusalem: 49*–67*.

Shneewer, H.A., Al-Loza, N.G., Kareem, M.A., and Hameed, I.H. 2015. Sequence Analysis of Mitochondrial DNA Hypervariable Region III of 400 Iraqi Volunteers. *African Journal of Biotechnology* 14(26): 2149–2156.

Skourtanioti, E., Erdal, Y.S., Frangipane, M., *et al.* 2020. Genomic History of Neolithic to Bronze Age Anatolia, Northern Levant, and Southern Caucasus. *Cell* 181(5): 1158–1175.

Stolarek, I., Handschuh, L., Juras, A., Nowaczewska, W., Kóčka-Krenz, H., Michalowski, A., Piontek, J., Kozlowski, P. and Figlerowicz, M. 2019. Goth Migration Induced Changes in the Matrilineal Genetic Structure of the Central-East European Population. *Scientific Reports* 9: 6737.

Van Oven, M. 2015. PhyloTree Build 17: Growing the Human Mitochondrial DNA Tree. *Forensic Science International: Genetics Supplement Series* 5: e392–e394.

Wang, C.C., Reinhold, S., Kalmykov, A., *et al.* 2019. Ancient Human Genome-Wide Data from a 3000-Year Interval in the Caucasus Corresponds with Eco-geographic Regions. *Nature Communications* 10(1): 590.

Weissensteiner, H., Pacher, D., Kloss-Brandstätter, A., Forer, L., Specht, G., Bandelt, H.-J, Kronenberg, F., Salas, A. and Schönherr, S. 2016. HaploGrep 2: Mitochondrial Haplogroup Classification in the Era of High-Throughput Sequencing. *Nucleic Acids Research* 44: W58–W63.

Young, K.L. 2009. *The Basques in the Genetic Landscape of Europe* (Ph.D. dissertation, University of Kansas). Lawrence.